

## DIFFUSION IN MAIN-SEQUENCE STARS: RADIATION FORCES, TIME SCALES, ANOMALIES

GEORGES MICHAUD\* AND YVES CHARLAND  
 Département de Physique, Université de Montréal

AND

SYLVIE VAUCLAIR AND GÉRARD VAUCLAIR  
 D.A.F. Observatoire de Meudon

Received 1976 March 8

### ABSTRACT

The abundance anomalies generated by diffusion in the envelope of main-sequence stars are studied. It is shown that in low-mass stars ( $M \lesssim 1.2 M_{\odot}$ ) diffusion leads to underabundances while in more massive stars ( $M \gtrsim 1.3 M_{\odot}$ ) diffusion leads to overabundances of at least some elements. In general the overabundance and underabundance factors generated (up to  $10^7$ ) are larger than the observed anomalies in stars of the main sequence (rarely up to  $10^6$ ). It is established that diffusion can lead to the largest anomalies observed. For particular elements (Sr, Eu, . . .), it is shown where more accurate calculations are needed. Approximate formulae are developed for radiative accelerations. They allow the reader to carry out calculations for cases of special interest to him and also to evaluate the uncertainty of the calculations.

*Subject headings:* stars: abundances — stars: interiors — stars: metallic-line — stars: peculiar A

### I. INTRODUCTION

Many of the slowly rotating stars of the upper main sequence [ $T_e > 7000$  K;  $T(K) \equiv 10^4 T_4$  in what follows] show abundance anomalies. In a few of the stars with  $1.0 < T_{e4} < 1.5$  some elements can be up to  $10^6$  times overabundant (Preston 1974, Fig. 7). The cooler stars show smaller anomalies (Smith 1973; Preston 1974).

A comparison of gravitational ( $g$ ) and radiative ( $g_R$ ) accelerations in the atmospheres of the hotter anomalous stars, and below the hydrogen convective zones for the cooler ones, shows that those elements which are pushed upward by the radiative force ( $g_R > g$ ) are overabundant, whereas those which settle down are underabundant. Most observed abundance anomalies can thus be explained in this zeroth-order model (Michaud 1970; Watson 1970, 1971a; Smith 1971; Michaud and Vauclair 1972; Vauclair, Michaud, and Charland 1974; Smith 1974; Michaud 1975).

However, the zeroth-order model only says that some elements will be overabundant and others underabundant. Can elements be pushed from deep enough in the interior of stars for overabundances of up to  $10^6$  to be generated? Why should the overabundance factors decrease as effective temperatures decrease below  $T_{e4} = 1$ ? Should there perhaps be smaller abundance anomalies in stars with  $T_{e4} = 0.6$ ? We shall here try to answer these questions. But this is only part of the problem. The generation of observable abundance anomalies depends on many factors

(see Michaud 1975 for a discussion): the state of the outer atmosphere (or outer boundary condition) (Michaud 1973; Michaud, Reeves, and Charland 1974), the turbulence in the zone where lines are formed and below, meridional circulation, the radiation forces in the atmosphere, and the migration of elements from the interior to the line-forming region. In this paper, we will concentrate on the last point, assuming no turbulence or meridional circulation, and always assuming that if elements are pushed to the atmosphere by radiation forces they will stay there and not leave the star. However, convection zones are taken into account. We obtain possible abundance anomalies in nonrotating stars. Any of the neglected aspects of the problem will tend to lower the abundance anomalies. In forthcoming papers we will study the effect of turbulence and meridional circulation, and we will do detailed radiation force calculations on a few elements of special interest (e.g., Li, Be, and B).

To carry out calculations throughout the stellar envelopes of main-sequence stars, we will develop (in § II) approximate formulae for radiation forces. We will apply them to the envelopes of 12 main-sequence stars. The formulae we present allow one to calculate approximate radiation forces rapidly for any element at any point where diffusion can be important in main-sequence stars (see Appendix B). Previously such radiation forces had been calculated for Am stars just below the convection zone by Watson (1971a) and over part of the envelope, for a few elements, by Kobayashi and Osaki (1973).

In § III we calculate the time evolution of abundance anomalies that diffusion produces on the surface of nonrotating stars of the main sequence. We determine

\* Partially supported by grants from Le Conseil National de Recherches du Canada and Le Ministère de l'Éducation du Québec.

how this varies along the main sequence for a large number of elements. For stars with  $M < 1.5 M_{\odot}$  we determine the size of anomalies and whether they materialize or not. For stars with  $M > 1.6 M_{\odot}$  we determine the size of anomalies; but, as discussed below, some may not materialize. Calculations of the time evolution of abundance anomalies have been carried out for Hg by Watson (1971*b*) and by Cowley and Day (1976). However, it is impossible from what Watson published to extend his calculations to other stars or elements and Cowley and Day's calculations appear very approximate, depending on only one point in the stellar envelope. In solar-type stars, Aller and Chapman (1960) determined time scales for diffusion but neglected radiation forces.

## II. RADIATION FORCES

In this paper, we are interested in obtaining general formulae which allow one to calculate approximate radiation forces for most elements of interest. First, the stellar envelopes used will be described, and then approximate radiation forces will be calculated, with complications added one by one which will make the results more accurate. The contribution of unsaturated lines will first be studied. For temperatures larger than  $4 \times 10^4$  K, elements generally will be shown to have their lines close to the maximum of the radiation flux except when they are in a *rare gas* configuration. However, elements of the iron peak or lighter are abundant enough for at least their resonance lines to be saturated. In § II*b*, we will investigate the effect of line saturation. The radiation force will then be drastically reduced. In § II*c* we will study the effect of the continuum. In § II*d* we apply the calculations of radiation forces to determine whether diffusion leads to overabundances in stars of the main sequence.

In a forthcoming paper, we will show that depending

on turbulence or laminar meridional circulation either He completely disappears, through gravitational settling, from the surface before most of the diffusion takes place or He remains on the surface for the whole life of the star while the diffusion of heavy elements goes on. In this paper we will study in detail the case when turbulence and meridional circulation are negligible. Helium then disappears rapidly, and the only convection zone that may exist is due to the ionization of hydrogen. Some diffusion of heavy elements will have occurred before the disappearance of the He convection zone; but because diffusion goes on much more rapidly below the hydrogen than below the He II convection zone, one may usually neglect the diffusion of heavy elements that occurred before the disappearance of He. Further, since the results of Vauclair, Vauclair, and Pamjatnikh (1974) have shown that the  $T(\rho)$  relationship is not appreciably affected by the diffusion of He, the radiation forces calculated in this paper may be used even if He is present. What will be changed by the presence of helium is the size of the mixed zone, which will include the He II convection zone, and so the surface abundances will be modified. The anomalies will generally be smaller.

The stellar envelopes used were calculated using a computer program (Martel 1974) based on the model of Paczynski (1969). The parameters of our models are listed in Table 1, in which  $\alpha$  is the ratio of mixing length to the pressure scale height. We used the opacities of Cox and Stewart (1970). In the envelopes, the helium abundance was assumed equal to zero. By comparing with the stellar atmospheres of Mihalas (1965) it was also found that the model envelopes gave, within 20 percent, the real  $T(\rho)$ ,  $M(\rho)$ , and  $T(\tau)$  relationships up to  $\tau_{4000} \approx 1$ . Of course, the radiation fluxes as a function of frequency are not properly calculated that far up.

The differential radiation pressure gradient transmitted to an element of atomic mass  $A$ , is, in the interior

TABLE 1  
PARAMETERS OF STELLAR MODELS

$M/M_{\odot}$	$T_{\text{eff}}(10^4 \text{ K})$	$g(10^4 \text{ cm s}^{-2})$	$T_4^*$	$\bar{\kappa} \dagger$	$\Delta M_c (\text{g cm}^{-2}) \ddagger$
5.0.....	1.62	1.14	...	6.3§	4.74-2
3.3.....	1.35	1.00	...	8.5§	3.36-2
3.3.....	1.35	1.90	...	11.9§	2.33-2
2.6.....	1.072	1.51	1.32	21.4	1.35-1
2.0.....	0.870	1.51	1.62	31.0	6.37-1
1.55.....	0.692	1.28	3.67	46.2	1.62+1
1.4.....	0.660	1.51	5.54	63.1	1.58+2
1.20.....	0.631	1.90	18.0	35.8	3.42+4
1.07.....	0.584	2.03	60.3	25.1	9.39+6
1.0 ( $\alpha = 1.0$ ).....	0.580	2.74	93.2	25.1	4.70+7
1.0 ( $\alpha = 1.5$ ).....	0.580	2.74	187	21.6	7.97+8
1.0 ( $\alpha = 0.7$ ).....	0.580	2.74	37.0	40.0	8.82+5

\* At the bottom of the convection zone.

† Rosseland mean opacity at the bottom of the convective zone.

‡ Mass (per  $\text{cm}^2$ ) in the convective zone or above an optical depth of 0.1.

§ At  $T_4 = 3.0$ .

of stars when  $\tau_\nu \gg 1$  at all frequencies,

$$F_\nu(A)d\nu = \frac{\pi T_{e4}^4 k^4 R^2 K_\nu(A) \bar{K}}{2c^3 h^3 r^2 X(A) K_\nu} u^4 \frac{e^u}{e^u - 1)^2} du$$

$$= 0.727 \frac{R^2 T_{e4}^4 K_\nu(A) \bar{K}}{r^2 X(A) K_\nu} P(u) du, \quad (1)$$

$$P(u) \equiv u^4 \frac{e^u}{(e^u - 1)^2}, \quad (1a)$$

where  $F_\nu(A)d\nu$  is the force transmitted through the differential radiation pressure in the interval  $d\nu$  to 1 gram of element  $A$  (in  $\text{cm s}^{-2}$ ).  $\bar{K}$  is the Rosseland mean opacity,  $K_\nu$  is the total opacity at frequency  $\nu$ , and  $K_\nu(A)$  the contribution of element  $A$  to  $K_\nu$ .  $R$  is the star radius, and  $r$  is the distance from the center of the star.  $X(A)$  is the mass fraction of element  $A$ ,  $T_{e4}$  is the effective temperature of the star in units of  $10^4$  K, and

$$u = 1.16h\nu/T_4, \quad (2)$$

where  $(h\nu)$  is in eV. Equation (1) was obtained from equation (4) of Vauclair, Michaud, and Charland (1974) from the radiation transfer equation and from the definition of the effective temperature. The correction  $[1 - \exp(-h\nu/kT)]$  for induced emission should be included in  $K_\nu(A)$  and  $K_\nu$  wherever appropriate. Equation (1) has the advantage of presenting ratios of opacities explicitly, thereby allowing a partial factoring out of approximations.

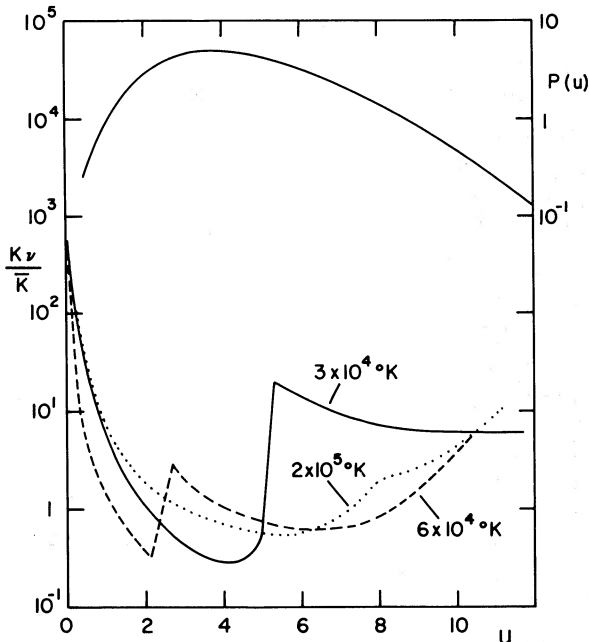


FIG. 1.—The function  $P(u)$  as a function of  $u = h\nu/kT$ , and the ratios  $K_\nu/\bar{K}$  for three different temperatures. The opacities at  $T = 3, 6,$  and  $20 \times 10^4$  K (respectively densities of  $1.35 \times 10^{-8}, 6.25 \times 10^{-8}, 4 \times 10^{-6}$   $\text{g cm}^{-3}$ ) were kindly calculated for us by Dr. A. N. Cox. The lines in his calculations were eye-averaged for this figure.

How do  $K_\nu/\bar{K}$  and  $P(u)$  vary in stellar interiors? On Figure 1 are plotted the ratios  $K_\nu/\bar{K}$  for three different temperatures:  $T_4 = 3, 6$  and  $20$ . At  $T_4 = 20$  and  $6$ , taking  $K_\nu/\bar{K} = 1$  leads in the interval

$$1.4 \leq u \leq 9.3 \quad (3)$$

to an error of less than a factor of 3. At  $T_4 = 50$  (not shown) it would be a factor of 2. At 3, there is no problem between

$$1.7 \leq u \leq 5.2, \quad (3a)$$

but above 5.2 the error is more like an order of magnitude. In our calculations of radiation forces, at  $T_4 > 4$  or 5, using  $\bar{K}/K_\nu = 1$  will not lead to errors larger than a factor of 3 but may lead to a factor of 10 overestimate of the radiation force at  $T_4 \sim 3$ . It may, however, be noted that in the calculations of time scales the more important portion of the star lies at the larger temperatures.

The function  $P(u)$  is also plotted on Figure 1. Its maximum is close to the maximum of  $\bar{K}/K_\nu$ . In the interval

$$1.5 < u < 8.0 \quad (4)$$

it varies by a factor of 2.0 from its average value of 3. It is the value used in most of our calculations. This will be described below in more detail. On a first reading, some may prefer to skip to the paragraph following equation (22).

#### a) Line Absorption

The radiation force transferred through bound-bound transitions is first obtained for *unabundant elements*. To this end, *lines* are assumed *unsaturated*. Then,  $K_\nu(A) \propto X(A)$ , and the ratio  $K_\nu(A)/X(A)$  (it is proportional to  $1/A$  but independent of  $\nu$ ) disappears from equation (1). From all states of ionization and excitation the sum of the  $f$ -values to all upper levels in the frequency range  $1.5 \leq u \leq 8.0$  is assumed equal to 1, i.e.,

$$\sum_m f_{nm} = 1, \quad (5)$$

where the sum is to be taken over all transitions from the level of interest  $n$ , to the upper levels  $m$ . Note that only the upper levels within the range of equation (4) are important. (See Appendix A for a discussion of  $f$ -values.) Also take  $K_\nu = \bar{K}$ , to obtain, after some manipulations,

$$g_R = 1.7 \times 10^8 \frac{T_{e4}^4 R^2}{AT_4 r^2} \text{ cm s}^{-2}, \quad (6)$$

where  $A$  is the atomic mass number of the element of interest. The  $T_4^{-1}$  dependence appears because as the temperature increases, the flux spreads over a larger energy interval and each line sees a smaller fraction of the total flux.

i) *Gravitational and Thermal Diffusion*

The radiative acceleration,  $g_R$ , is to be compared with

$$g \approx 1.5 \times 10^4 R^2/r^2 \text{ cm s}^{-2}, \quad (7)$$

the acceleration due to gravity in main-sequence stars, and to a thermal diffusion term. To obtain the thermal diffusion contribution, use the diffusion equation (Montmerle and Michaud 1976), replacing the temperature gradient term as done above to obtain equation (1). The acceleration due to gravity may then be replaced by an effective acceleration

$$g_{GT} = g \left[ 1 + \frac{3}{8} \frac{3.45Z^2 - 0.8Z}{(2A - Z - 1)g} T_{e4}^4 \bar{K} a T_4^{0.36} \right] \quad (8)$$

that takes thermal diffusion into account. The diffusion equation used is appropriate to trace elements diffusing in hydrogen (Aller and Chapman 1960; Burgers 1960; Montmerle and Michaud 1976). The only approximation made was in using equation (9) for  $p_e$ . The thermal diffusion term depends on  $Z$ , the degree of ionization, and will vary from element to element at a given position in the star and, for the same element, will depend on the distance from the star center. The acceleration needed to counter gravity and thermal diffusion ( $g_{GT}$ ) is shown on Figure 2 for Mn in the envelope of a  $2.0 M_\odot$  star. The ionization potentials were taken from Allen (1963) or, when not available there, from Carlson *et al.* (1970) or Kelly and Harrison (1971). At high temperature Figure 2 shows that thermal diffusion is more important than that due to gravity. This will be especially important for the Sun (see § II d).

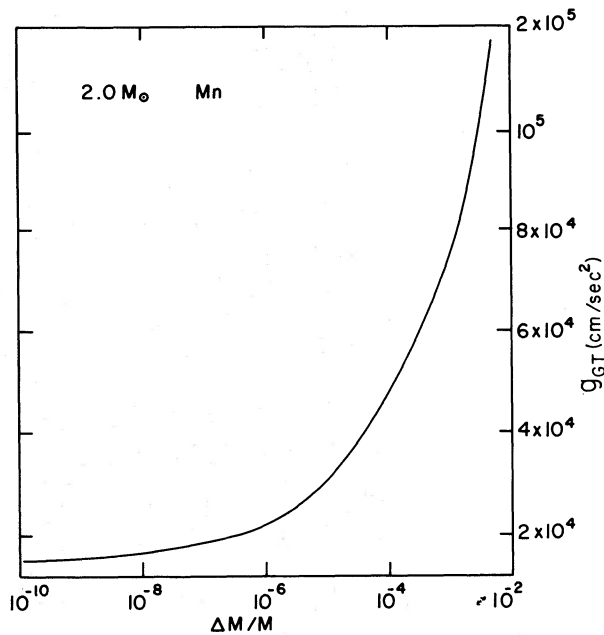


FIG. 2.—The acceleration,  $g_{GT}$ , needed to counter gravity and thermal diffusion on Mn in a  $2 M_\odot$  stellar envelope.  $\Delta M/M$  is the fraction of the mass of the star above the point of interest.

ii) *Line Position versus Radiative Flux Maximum*

When is it reasonable to assume equation (6), and when is it clearly an overestimate even for trace elements, i.e., even when there is no saturation of lines? The main assumption in obtaining equation (6) is then that the element of interest has lines with large  $f$ -values in the interval where  $P(u) \approx 3$ , i.e., in the frequency range of the flux maximum. We will show that for the temperatures where the Lyman jump is weak ( $T_4 \gtrsim 4$ ) this condition is also met. The value of  $u$  at which an element generally ionizes is first determined using an approximate relation between the temperature and the electron pressure in the star. From our model envelope calculations

$$p_e = a T_4^{4.36} \quad (9)$$

and

$$\frac{\Delta M}{M} = c T_4^d \quad (10)$$

were obtained. The quantities  $a$ ,  $c$ , and  $d$  are given in Table 2 as a function of the stellar mass. Equations (9) and (10) are accurate to a factor of 1.35 for the electron pressure for  $\tau_{\text{Rossel}} \geq 10$  for the  $M = 5.0$ , 3.3, and  $2.6 M_\odot$  models and below the convection zones for the other models. The equations are valid down to  $T_4 \sim 140$ . Then using Saha's equation, it is easy to show that

$$\frac{\chi_{I-1}}{kT} = u_{I-1} = 22.62 - 2.3026 \left( \log_{10} \frac{N_I}{N_{I-1}} \frac{B_{I-1}}{B_I} a \right) - 4.283 \log_{10} T_4, \quad (11)$$

where  $B_{I-1}$  and  $B_I$  are the partition functions. Now let us define

$$b_I = \frac{\chi_I}{\chi_{I-1}} \quad (12)$$

as the ratio of two successive ionization potentials. A survey of ionization potential tables (Allen 1963 or,

TABLE 2  
PARAMETERS FOR  $p_e$  AND  $\Delta M/M$  (EQS. [9] AND [10])

$M/M_\odot$	$a$	$c$	$d$
5.0	$1.00 \times 10^3$	$1.67 \times 10^{-12}$	4.16
3.3 ( $\log g = 4$ )	$1.33 \times 10^2$	$2.70 \times 10^{-12}$	4.16
3.3	$1.90 \times 10^2$	$1.27 \times 10^{-12}$	4.16
2.6	$2.4 \times 10^2$	$2.77 \times 10^{-12}$	4.16
2.0	$4.0 \times 10^2$	$4.14 \times 10^{-12}$	4.16
1.55	$5.3 \times 10^2$	$6.84 \times 10^{-12}$	4.16
1.4	$7.75 \times 10^2$	$6.07 \times 10^{-12}$	4.16
1.2	$9.7 \times 10^2$	$5.0 \times 10^{-11}$	3.6
1.07	$1.25 \times 10^3$	$3.2 \times 10^{-10}$	3.3
1.00*	$1.55 \times 10^3$	$2.6 \times 10^{-10}$	3.3

\*  $\alpha = 1$ .

when not available there, Carlson *et al.* 1970 or Kelly and Harrison 1971) shows

$$b_I \approx 2 \quad (13)$$

for  $\chi_{I-1} \leq 30$  eV or when  $\chi_I$  has a closed shell configuration. In the other cases,

$$b_I \approx 1.3. \quad (14)$$

Further, a survey of the position of first excited levels in Moore's tables shows that, for ionized elements, they are generally at less than 30 percent of the ionization potential except for closed shell configurations or configurations with one electron less than a closed shell. Then for ionized elements, with  $\chi_I > 50$  eV ( $\chi_{I-1} > 30$  eV) but not in a rare gas configuration, the first excited level will be at

$$\begin{aligned} 0.3\chi_I/kT &= 0.4 u_{I-1} \\ &= 3-6.6. \end{aligned} \quad (15)$$

To obtain equation (15), equations (11) and (12) were used with  $B_{I-1} = B_I$  and  $N_{I-1} = N_I$  for ionization of half of the elements at  $T_4 \geq 2.2$ . But from Figure 1 this is the range of the maximum of  $P(u)$ . For most cases then there are excited levels positioned within the maximum of  $P(u)$  which will lead to lines from the ground state. The exceptions are for  $\chi_{I-1} \leq 30$  eV, and for rare gas configurations. Elements with ionization potentials of 30 eV, however, generally ionize at  $T_4 \approx 2.4$ . The most stringent conditions for the accuracy of these calculations is then that the Lyman jump be small, or  $T_4 \geq 4$  as determined below equation (3).

### iii) Rare Gas Configuration

The effect of rare gas configurations requires further study. Let  $E_I$  be the ratio of the energy of the first excited level to the ionization potential of the rare gas; then the first line will have

$$u_{1st\ line} = b_I E_I u_{I-1}. \quad (16)$$

On Figure 3,  $b_I E_I$  is given for two cases. For a factor of 10 reduction, the radiation force to state  $I$  must be reduced by a factor of 10 when state  $I-1$  is 90 percent ionized. That is,

$$P(u_{1st\ line}) = 0.3, \quad (17)$$

or  $u_{I-1} = 10.7/b_I E_I$ . To determine  $b_I E_I$ , use equation (11) with  $N_I = 10N_{I-1}$  and take into account that for rare gases,  $B_I \approx 0.5B_{I-1}$  and  $B_{I+1} \approx 10B_I$ . A survey of Moore (1949, 1952, 1958) shows this to hold within approximately a factor of 1.3. We so obtained Figure 3 for  $b_I E_I$  as a function of temperature for a  $2 M_\odot$  star. For other reduction factors, one may similarly return to equation (11).

Merely by looking at tables of ionization potentials and excitation levels, one can immediately determine for any element how large the reduction of the radia-

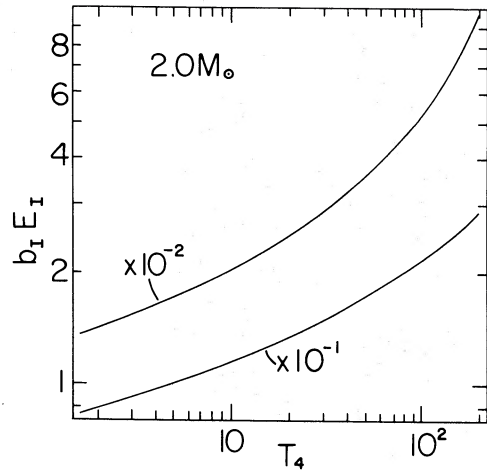


FIG. 3.—Minimum energy of the first excited level of a rare gas for a factor of 10 and a factor of 100 reduction in the radiative acceleration, in units of the ionization potential of the preceding element.

tion force can be for rare gas configurations. Before proceeding to calculations of radiation forces, one additional effect must be described.

### iv) Radiative Acceleration for Unabundant Elements<sup>1</sup>

Where many states of ionization are simultaneously present for a given element, some care has to be taken in the redistribution of the radiation force. The effect is especially important in stellar atmospheres or upper stellar envelopes because of the large difference between the diffusion coefficient of the first few ionization states. We have included this effect in our calculations using for the average radiation force (Montmerle and Michaud 1976)

$$\begin{aligned} g_R &= \frac{1}{\bar{D}} \sum_I D_I \frac{N_I(A)}{N(A)} \frac{\beta_{colI}}{\beta_{ionI} + \beta_{colI}} g_{RI} \\ &+ \sum_I \frac{N_I(A)}{N(A)} \frac{\beta_{ionI}}{(\beta_{ionI} + \beta_{colI})} g_{RI}, \end{aligned} \quad (18)$$

where

$$\bar{D} = \sum_I N_I(A) D_I / N(A),$$

$$\beta_{colI} = \frac{kT}{mD_{pI}},$$

and  $\beta_{ionI}$  was calculated using the hydrogenic approximation (Spitzer 1968; Michaud 1970). Here  $m$  is the mass of particle  $A$ , and  $g_{RI}$  was taken from equation (6) for all states of ionization except those that are either in the rare gas state or have one electron less

<sup>1</sup> By unabundant elements we will mean those whose radiative forces are unaffected by the saturation of the radiative flux.

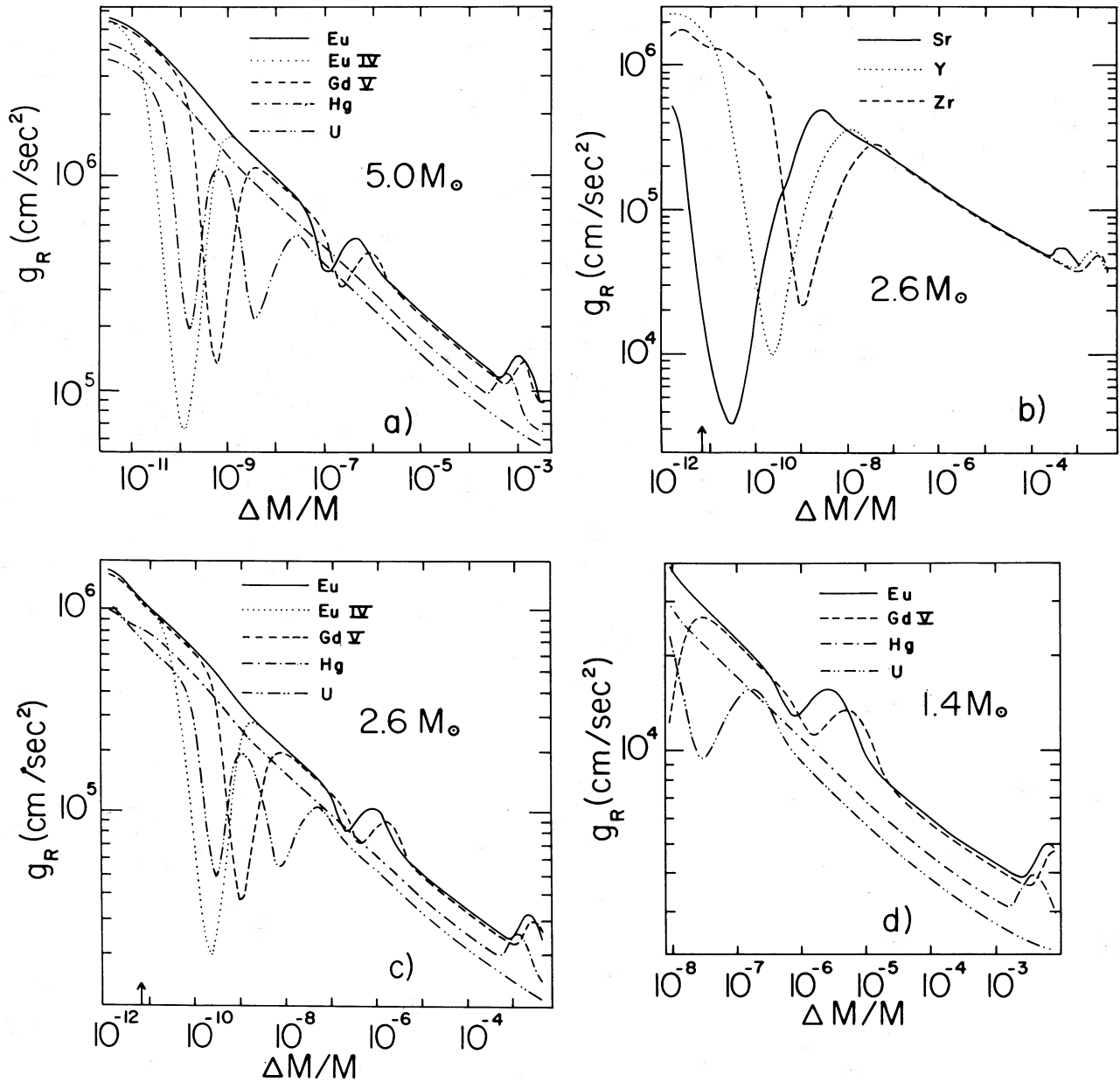


FIG. 4.—Radiative acceleration as a function of the fraction of the stellar mass above the point of interest. No saturation of the radiation flux occurs for these elements. From parts (a), (c), (d), and (e) it appears that whereas heavy elements are clearly pushed upward in the more massive stars, they may or may not be pushed upward in a  $1.4 M_\odot$  star and they are certainly not pushed upward in the Sun. The vertical arrows on part (e) indicate the bottom of convection zones for  $\alpha = 0.7, 1.0,$  and  $1.5$ . The dips in the Eu IV, Gd V and U curves assume rare-gas configurations for the IVth configuration of Eu and the Vth configurations of Gd and U. On part (b) note the different behavior of Sr, Y, and Zr. It probably explains variations in the abundances of these elements from star to star. Depending on whether diffusion occurs below the hydrogen convection zone (indicated by an arrow) or throughout the atmosphere (the weak convection could be stabilized by a magnetic field), strontium is either underabundant or overabundant. Finally, on part (f) is shown the effect of assuming that all the states of ionization of Eu have a rare-gas-like configuration.

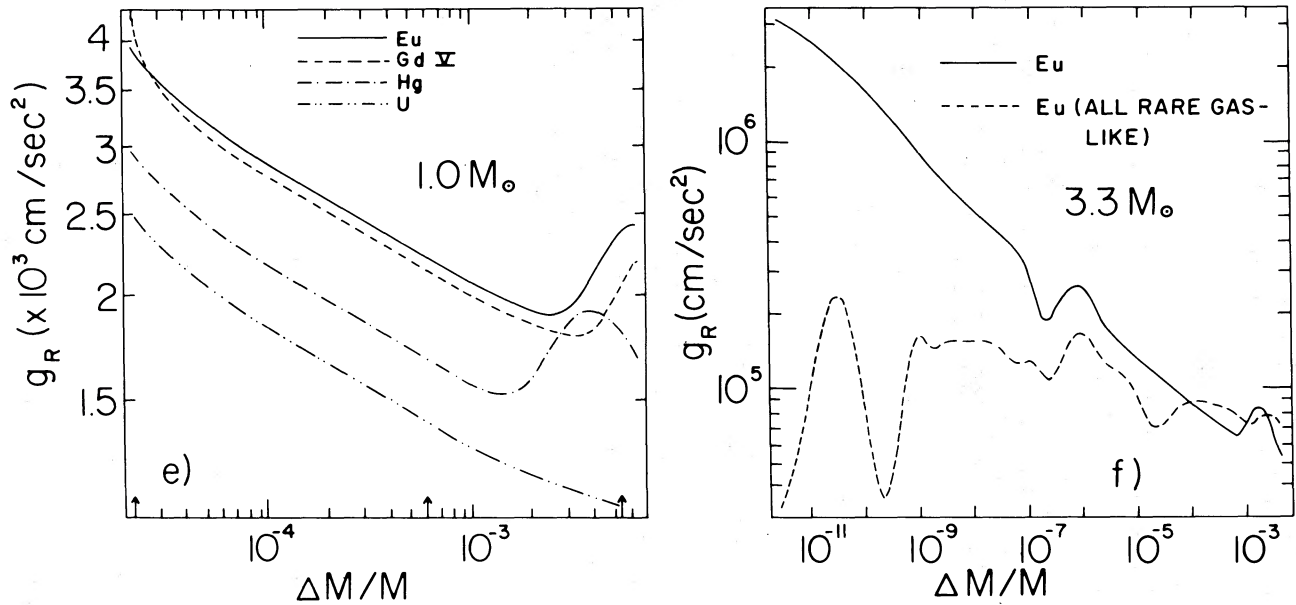


FIG. 4.—Continued

than a closed shell. For rare gases,  $g_{RI}$  was taken as

$$g_{RI} = 1.7 \times 10^8 \frac{T_{e4}^4 R^2 P(u_{rg})}{AT_4 r^2 3}, \quad (19)$$

where

$$u_{rg} = b_l E_l u_{l-1} = 0.6 \chi_l / kT. \quad (20)$$

The function  $P(u)$  was defined after equation (1). Using equation (20) is equivalent to assuming that for rare gases, the lines start appearing at around  $0.5\chi_l$ . A survey of Moore (1949, 1952, 1958) indicates that this probably leads, on the average, to a slight underestimate of the radiation forces for rare gases. For states of ionization with one electron less than a rare gas, equation (19) with equation (20) replaced by

$$u = 0.5\chi_l / kT \quad (21)$$

was used. Finally the uncertainty in the assumed averaged radiation flux was estimated by carrying out calculations using equations (19) and (20) for *all* states of ionization. The results for this calculation are shown with dashed lines on Figure 4f. It appears that for  $T_4 > 10$  ( $\Delta M/M = 10^{-8}$ ) the effect is relatively small. At  $T_4 = 5$ , it is a factor of 5.

These calculations will be most accurate for  $T_4 \geq 4$ . Then the Lyman jump is smaller, and elements with  $\chi_{l-1} = 50 \text{ eV}$  are half-ionized, so that one can assume  $b_l \leq 1.3$  except for rare gases. For most elements, equation (19) may then be expected to be within a factor of 2 of an upper limit and a factor of 5 of a lower limit. The lower limit could be that low if, from the various levels

$$\sum_m f_{nm} = 0.2 \quad (22)$$

instead of equation (5). All this applies to unimportant elements whose lines are unsaturated.

A few of the calculated radiation forces are shown on Figure 4. First note that in the more massive stars, there is no doubt that the unimportant heavy elements will be pushed upward. The radiative accelerations are larger than the gravitational and thermal accelerations by many orders of magnitude. Second, note the strong dips that occur for certain elements. They are due to rare-gas configurations and to the jump in ionization potentials that occur for rare gases. Note the two curves for europium in a  $2.63 M_{\odot}$  star (Fig. 4c). That merely labeled europium was calculated assuming that europium was in the configuration of a rare gas (xenon) when it had lost nine electrons. No dip occurs because the difference in ionization potentials is too small there (Carlson *et al.* 1970). However, the curve labeled europium IV was calculated assuming that when europium has lost three electrons it is in a rare-gas configuration. This causes a deep dip (at  $T_4 \sim 3$ ,  $\Delta M/M \sim 2.7 \times 10^{-10}$ ) in the radiative acceleration because of the relatively large jump in ionization potential (from 22 to 54 eV). The calculations of Carlson *et al.* (1970) indicate that, for rare earths, the large jumps in ionization potential occur not in the xenon configuration, but much earlier. The atomic physics of rare earths appears too poorly known for us to know whether such configurations resemble rare gases with their lack of low energy levels. Until this is cleared up, the diffusion calculations for rare earths will be very uncertain. It may well be that variations in abundance anomalies from one rare earth to the next will be explained by the atomic physics of the configuration for which the jump in ionization potential occurs. Until the states of ionization important at

$T_4 \sim 3$  are well studied, it will be impossible to determine the detailed abundances of rare earths in the atmosphere. However, at higher temperatures, deeper in the star, this effect does not come in since the ratio of successive ionization potentials is too close to 1. For most heavy elements then, radiation pressure will cause overabundances in stars of  $1.55 M_\odot$  or more; however, a few elements will not be pushed as far as the atmospheres because of their atomic structure at  $T_4 \sim 3$ . It is a region that must be studied in detail in future studies.

Note also the importance of the dip on the radiative acceleration of strontium. In the  $2.6 M_\odot$  model depending on whether diffusion occurs below the hydrogen convection zone (indicated by an arrow on Fig. 4b) or whether the hydrogen convection zone is stabilized by a magnetic field, strontium will be underabundant or only slightly overabundant.

b) The Effect of Saturation

If in equation (1)

$$K_\nu(A) \approx K_\nu \tag{23}$$

for some lines, those lines are saturated and the above estimates are large overestimates. This occurs for iron-peak and lighter elements. For those elements, line profiles will have to be integrated in detail and the number of lines of given  $f$ -values available from each state in the atom will be important. We first describe the Doppler line profile calculations made and then how they change if Lorentz line profiles are used. We so determine a measure of the uncertainty of the calculations

Even when lines are saturated, the above analysis of the  $P(u)$  function in equation (1) remains valid (see § IIa). However, the analysis of  $K/K_\nu$  has to be carried out again. Define  $K_\nu(A)$  and  $K_\nu(P)$ :

$$K_\nu = K_\nu(A) + K_\nu(P), \tag{24}$$

where  $K_\nu(A)$  is the part of the monochromatic coefficient of opacity due to the lines of interest and  $K_\nu(P)$  the opacity coefficient exclusive of the lines of interest. Assuming that the lines do not overlap,

$$\begin{aligned} K_\nu(A) &\approx \frac{1}{\rho} N_n(A) \sigma_{nm} \\ &= 0.0265 \frac{N_n(A)}{\rho} f_{nm} g_\nu, \end{aligned} \tag{25}$$

where  $\sigma_{nm}$  is the absorption cross section at the frequency of interest, for the transition of interest and  $g_\nu$  is the line profile,

$$g_\nu = \exp [-(\nu - \nu_0)^2 / \Delta\nu_D^2] / \Delta\nu_D \sqrt{\pi}, \tag{26}$$

$$\Delta\nu_D = \frac{1}{c} \left( \frac{2k}{m_p} \right)^{1/2} \left( \frac{T}{A} \right)^{1/2} \nu_0 \tag{27}$$

for Doppler broadening, which is the first one discussed

here. For unsaturated lines,  $K_\nu(A)$  is much smaller than  $K_\nu(P)$ , and the denominator of equation (1) is the same from all levels  $m$  to all levels  $n$ . Physically, for unsaturated lines, the radiation flux is the same for all lines. It is then possible to sum over  $n$  and  $m$  and consider only  $\sum_n N_n$  and  $\sum_m f_{nm}$ , which is what was done (see § IIa) for unsaturated lines. Not here, however; depending both on  $f_{nm}$  and on  $N_n$ , some transitions will be saturated and others will not. The width of the line will also enter through  $g_\nu$ . The force transferred through each line has to be calculated *before* the summation can be done over  $n$  and  $m$ . Each level and each line must be considered separately.

To determine the occupancy of levels,  $N_n$ , for Doppler line calculations, we used the Mn I-v configurations. The excitation energy and statistical weight of each level (Moore 1949) were used to determine the number of levels important in the radiation force calculations. We stopped at configuration v, since the atomic data were becoming too incomplete. From each level, the transitions used were those determined in Appendix A. Equation (1) was integrated numerically over the Doppler line profile for each value of  $f_{nm}$  and for every level of Mn I to Mn v. The summations were then carried out over  $n$  and  $m$  to obtain the saturated radiation forces. The calculations were carried out for all temperatures within

$$1.5 < T_4 < 5 \tag{28}$$

in the  $3.3 M_\odot$  envelope, and for

$$10^{-13} \leq X(M_n) \leq 10^{-3}. \tag{29}$$

The results were *then fitted* to the formulae:

$$g_{RIs} = g_{RI} E \frac{BK T_4^{3/2} A^{1/2}}{BK T_4^{3/2} A^{1/2} + 7.1 \times 10^2 X_I(A)/X_0} \tag{30}$$

with

$$B = \left[ 1 + \frac{X_I^{0.36}(A)}{X_0^{0.36}} \right] \tag{31}$$

and

$$X_I(A) = N_I(A) X(A) / N(A).$$

$I$  designates the state of ionization.  $X_0$  and  $E$  are listed in Table 3 for the different approximations of Appendix A. It is described in Appendix C how one can arrive at equation (30). The quantity  $g_{RI}$  is the one

TABLE 3  
PARAMETER OF SATURATED FORCES (EQS. [30] AND [31])

	$X_0$	$E$
Middle.....	$3 \times 10^{-7}$	1.0
High.....	$1.5 \times 10^{-6}$	2.0
Low.....	$1.5 \times 10^{-6}$	0.2

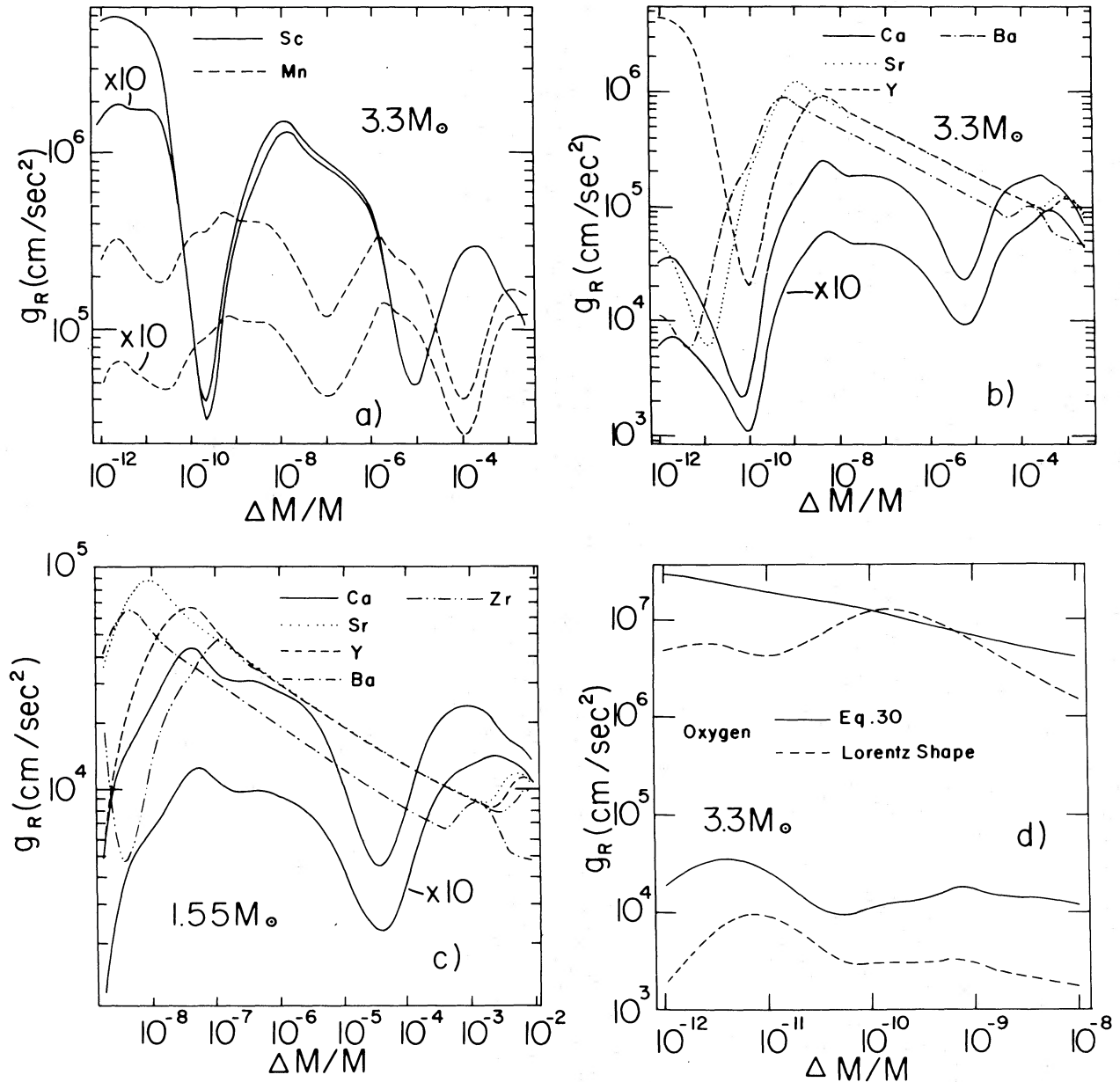


FIG. 5.—Radiative acceleration of abundant elements, as a function of the fraction of the stellar mass above the point of interest. Saturation of the radiative flux occurs for Mn and Ca, for which radiative accelerations were calculated both for a natural and 10 times a natural abundance (labeled  $\times 10$ ). On part (a) is shown the effect of saturation on two elements near iron. On parts (b) and (c) it appears that part of the different behavior of Sr and Ca is due to saturation. The two elements have very similar ionization potentials, but calcium has a much larger natural abundance which leads to saturation of the radiation flux. Compare Sr, Y, and Ba. In one star a given element may be overabundant, whereas in another star it is the other element which is overabundant. On part (d) of the figure are compared the radiation forces on oxygen calculated with our average formula (eq. [30]) and with Lorentz profiles. See the text. The two upper curves are for negligible abundances of oxygen whereas the two lower curves are for "natural" abundances.

determined for unsaturated lines (equation [6] or [19]).

The calculated radiation forces are shown on Figure 5 for a few cases of saturated radiative fluxes. Take, for instance, the case of manganese in a  $3.3 M_\odot$  star

(Fig. 5a). The radiative accelerations for a "natural"<sup>2</sup> and 10 times above a natural abundance are shown.

<sup>2</sup> For the "natural" abundances we used those determined by Cameron (1973) except that his boron abundance was reduced by a factor of 10.

Saturation is most important close to the surface. It has less effect when temperature increases. The deep dips in the radiative acceleration at  $\Delta M/M = 10^{-7}$  and  $10^{-4}$  are due to rare-gas configurations. Radiative acceleration pushes manganese upward from as deep as  $\Delta M/M = 10^{-4}$  (since there  $g_R \sim g_{GT}$ ). If manganese were 100 times overabundant (which is about the natural abundance of iron), the upward and downward accelerations would be about equal. On Figures 5b, 5c, and 5d are shown the behavior of Ca, Sr, and Ba in a few stellar masses of interest. Part of the different behavior of those elements in peculiar stars is certainly due to saturation effects: calcium is more abundant to start with. However, the cancellation of the upward and downward acceleration is very close in some areas of the star, and more detailed calculations are needed (Praderie and Michaud, in preparation).

To obtain an estimate of the uncertainty, other calculations were carried out, but for the configurations I to V of oxygen, and with Lorentz profiles instead of Doppler profiles. The full line width at half-maximum was taken from Griem (1960):

$$\Delta\nu_L = 8 \times 10^{15} (n_n^4 + n_m^4) \rho / (Z + 1)^2 \text{ s}^{-1}, \quad (32)$$

where  $n_n$  and  $n_m$  are the principal quantum number of the lower and upper levels, respectively,  $\rho$  is the density ( $\text{g cm}^{-3}$ ), and  $Z$  the degree of ionization of the element of interest. The principal quantum numbers were raised to the fourth instead of the fifth power since the number of levels considered is here larger than in hydrogenic configurations (see also Cox 1965). The constant appearing on the right-hand side of equation (32) is not that determined by Griem (1960) but was obtained by requiring that, on the average, our expression for  $\Delta\nu_L$  give the same width as the 38 widths calculated by Chapelle and Sahal-Br  chot (1970) and by Sahal-Br  chot and Segre (1971). The approximate expression for  $\Delta\nu_L$  was so normalized to their more exact calculations. The  $f_{nm}$  values were again taken from Appendix A. However,  $P(u)$  was not assumed equal to 3 but was explicitly calculated for each line at each point in the star. The needed energy differences between levels  $n$  and  $m$  were taken from Moore (1949); and after a survey through Wiese, Smith and Miles (1969), it was decided to give the largest  $f_{nm}$  value to the transition with the smallest  $\Delta\nu_{nm}$  which was allowed in Russell-Saunders coupling (see, e.g., Herzberg 1944). The other  $f_{nm}$  values were allocated to higher levels,  $f_{nm}$  decreasing as the energy increased. The only transitions included were those allowed in Russell-Saunders coupling. The forces calculated in this way are compared with our fitting formula (eq. [30] on Fig. 5d). Both at negligible abundances ( $X_0 = 10^{-14}$ ) and at the "natural" abundance of oxygen our fitting formula gives systematically larger radiative accelerations than the pressure-broadened calculations by approximately a factor of 3. It is mainly due to two factors: the lighter elements, like oxygen, do not have quite so many energy levels as manganese does; and the levels of oxygen do not, on the average, lead to

lines so well placed in the spectrum as assumed in obtaining equation (30). This will be true, in general, for the lighter elements, and we probably overestimate somewhat the radiative acceleration of the abundant light elements like C, O, Ne, . . . , but not of iron-peak or heavier elements. Part of the disagreement is, however, related to our using only Doppler widths, and Doppler profiles, for equation (30), and only pressure broadening, and Lorentz profiles, for the comparison calculation. Equation (32) gives widths 100 times smaller than Doppler widths. Using Voigt profiles instead of Lorentz profiles would have somewhat reduced the disagreement of radiative accelerations. At the same time, however, our using only Doppler widths and profiles is implicitly justified.

### c) The Contribution of the Continuum

In the interior of stars, the radiation force transmitted through the continuum is always relatively small except for helium or other very light elements. It can be estimated by using equation (1) and the hydrogenic approximation, the Saha equation, and equation (9) for  $p_e$ . Further, usually the radiation force transmitted through ionization of the  $Z$ th state is maximum when the element is mainly in the  $(Z + 1)$ th state of ionization. Then, if  $\bar{K} = K_v$ :

$$\begin{aligned} g_{\text{con}} &= \int F_v(A) d\nu \\ &= 5.57 \times 10^{-4} u_l^4 T_{e4}^4 a T_4^{1.86} \frac{n}{A(Z+1)^2} \frac{R^2}{r^2} \text{ cm s}^{-2}, \end{aligned} \quad (33)$$

where  $u_l = \chi_l/kT$ . The element must be mainly in the state  $I + 1$ . The quantity  $a$  is given in Table 2, and  $n$  is the principal quantum number of the level from which ionization occurs.

Use as a rough approximation:  $u_l \approx 10$ ,  $a \sim 5 \times 10^2$ ,  $n = 3$ ; the  $T_4$  and  $Z$  terms nearly cancel for many heavy elements:

$$g_{\text{con}} = 8.4 \times 10^3 T_{e4}^4 R^2 / (Ar^2) \text{ cm s}^{-2}, \quad (34)$$

so that only for relatively small  $A$  (He for instance) and high  $T_{e4}$  could the continuum be of any importance. Compare with equation (6): the force through the continuum is much smaller than the force through unsaturated lines. We will neglect the contribution of the continuum in what follows.

### d) Abundance Anomalies

The calculated radiation forces will now be used to determine what abundance anomalies are to be expected in stars on the main sequence. The reader wishing to carry out such calculations may refer to Appendix B. The time scales will be discussed in the next section. Results for  $1 M_\odot$  stars will first be presented: it is the simplest case. As the stellar mass increases, the analysis will become more and more complicated; diffusion proceeds closer and closer to the surface and then, at

lower temperatures, the radiation forces are more sensitive to the details of the flux and to the details of the atomic physics of each element. We specify models by their mass. However, the most important aspect of the envelope models is the temperature at the bottom of the convection zone. In turn, that temperature depends directly not on the mass of the star but on its effective temperature. In a  $1.2 M_{\odot}$  star, model envelopes for  $T_{\text{eff}} = 0.631$  and  $0.651$  show that increasing the effective temperature by 3 percent decreases the temperature at the bottom of the convection zone by a factor of 2. When relating our results to observations one should then do it through the effective temperatures given in Table 1, for every model. Note that a 3 percent change in effective temperature will then completely change the anomalies through the factor-of-2 change in the temperature at the bottom of the convection zone.

By un-abundant elements we will mean those whose radiative forces are unaffected by saturation of the radiative flux. For all the stars considered, *Lithium, beryllium, boron, scandium, and elements heavier than zinc in "natural" abundance are not affected by saturation.* V, Cu, and Zn are marginally affected. Elements

heavier than Zr must be some 100 times overabundant in the reservoir before they are affected by saturation.

In solar mass stars, diffusion leads to underabundances of all elements. All elements except fluorine have a radiation force more than 10 times smaller than the downward term,  $g_{\text{GT}}$  (see Fig. 4e at the middle arrow). The underabundance then appears well established. However, this conclusion is based on using  $\alpha = 1.0$  for our calculations of the envelope, where  $\alpha$  is the ratio of mixing length to the pressure scale height. If  $\alpha = 1.5$ , the underabundances are even more strongly established (arrow to the right on Fig. 4e). However, we also carried calculations at  $\alpha = 0.7$  (arrow to the left on Fig. 4e). The radiative accelerations are still smaller than  $g_{\text{GT}}$  for all elements. However, for B the two are nearly equal; and for Be, Na, Al, P, and K they are within a factor of 5. Unless  $\alpha$  were appreciably smaller than currently believed, diffusion would lead to underabundances of all elements in solar-type stars. The main uncertainty is due to our poor understanding of the hydrodynamics. Note that for  $\alpha = 1.0$ ,

$$g_{\text{GT}} \approx 3g,$$

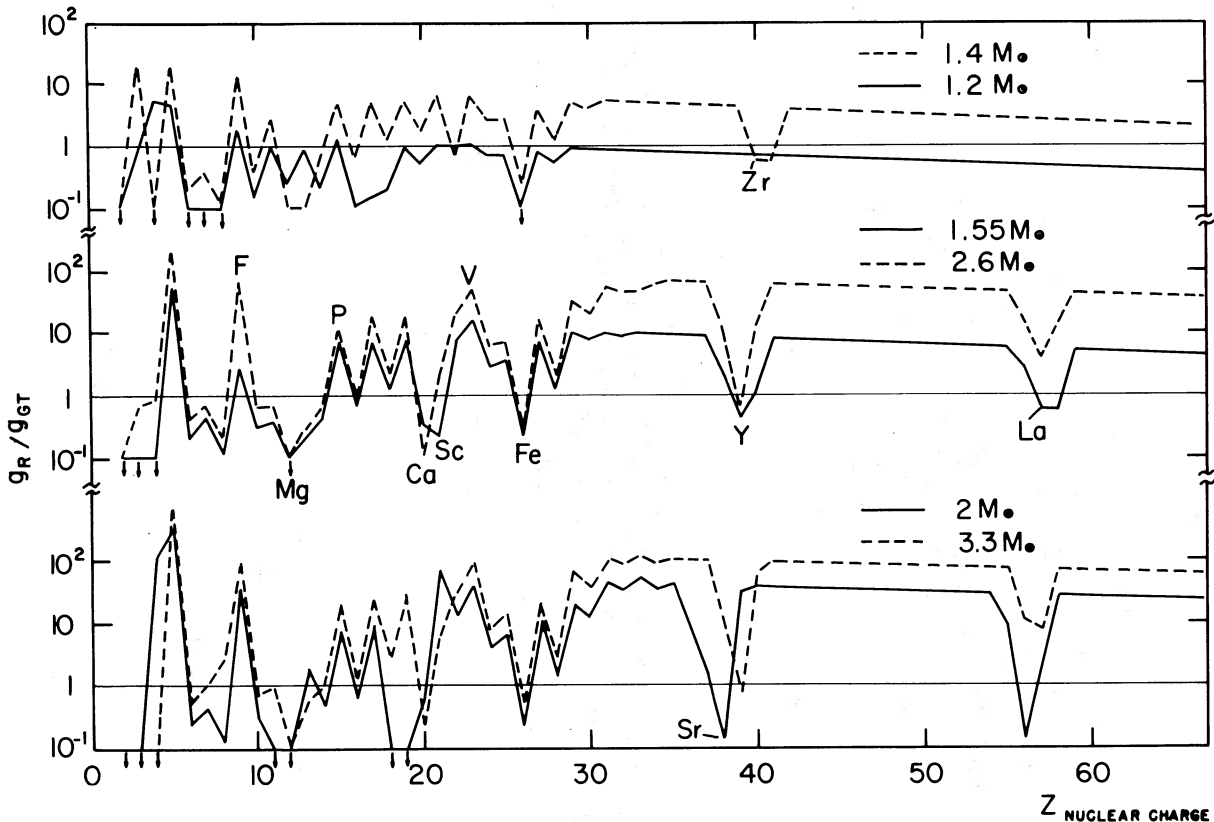


FIG. 6.—Ratio of upward (radiative) acceleration to downward acceleration (gravitational modified by the temperature gradient) for all elements in main-sequence stars. In this figure,  $Z$  is the nuclear charge. The uncertainty of these calculations being a factor of 5, it is clear that in stars of  $1.5 M_{\odot}$  or more, most heavy ( $A \geq 60$ ) elements are pushed upward. Note that in the  $2.6$  and  $3.0 M_{\odot}$  stars, the calculations were made at  $T_4 = 3.0$ , and not at the bottom of the convection zone or in the atmosphere. Diffusion between  $T_4 = 3.0$  and the surface will modify these results and will depend sensitively on the detailed atomic structure of each of the first few stages of ionization of each element.

since most of the downward diffusion is due to thermal diffusion. The time scales for the development of underabundances will be discussed in the next section.

For the  $1.07 M_{\odot}$  star, the radiative acceleration is still lower than  $g_{\text{GT}}$  for all elements; however, they are within a factor of 5 of each other for some of the less abundant elements below the iron peak even for  $\alpha = 1.0$ . As can easily be verified using equations (6) and (8), even the unsaturated forces are, for iron-peak elements, more than 5 times smaller than the accelerations needed to counter gravity and thermal diffusion. If affected by diffusion, iron-peak elements will be underabundant in such stars.

In the  $1.2 M_{\odot}$  star (see Fig. 6; the  $g_{\text{R}}/g_{\text{GT}}$  ratios were calculated at the bottom of the H I convection zone for the 1.2, 1.4, 1.55, and  $2 M_{\odot}$  stars) the upward and downward accelerations are nearly equal for those of the iron-peak elements that are un-abundant. C, N, O, S, and Ar are underabundant both because of saturation and because of ionization effects. Chlorine is underabundant because of ionization effects. Elements heavier than iron will generally be underabundant. A few of the un-abundant light elements will probably be overabundant.

In the  $1.4 M_{\odot}$  star, the unsaturated radiation forces become large enough to push even the heaviest elements upward (see Fig. 6). If an un-abundant element is not in the configuration of a rare gas at the bottom of the convection zone, it will be pushed upward and will be overabundant. Further, if  $A \lesssim 60$ , the radiative acceleration will be more than 5 times the downward acceleration. It is the case for Li, B, F, Cl, K, Sc, V, and Co. These elements should be overabundant. Another group of elements will certainly be underabundant: He, C, O, Mg, and Al. The radiation forces on Be, Mg, and Al are strongly influenced by the weakness of the radiation forces in rare gas configurations. For the other elements the upward and downward accelerations are within a factor of 5 of each other, and it is somewhat uncertain which will win.

All un-abundant elements, in particular all elements heavier than iron, will be pushed upward in the  $1.55 M_{\odot}$  and heavier stars unless they are in a rare gas configuration or affected by the Lyman jump at the bottom of the convection zones. In a  $1.55 M_{\odot}$  star, above the iron peak, only La and Y are strongly affected by rare gas configurations and are underabundant. For the more abundant iron-peak elements, Cr, Mn, Fe, and Ni, the upward diffusion is affected by saturation of the radiation field and is within a factor of 5 of downward diffusion. Most of them should, however, be overabundant. V and Ti will be overabundant while Mg, Ca, and Sc are strongly affected by rare gas configurations and will be underabundant. So also are Li and Be. Oxygen will be underabundant because of saturation of the lines. The other un-abundant light elements, B, P, Cl, and K, will be overabundant. For the other light elements, upward and downward diffusion will be within a factor of 5 of each other.

These calculations neglect the effect of the Lyman jump. It is likely to be important for some elements in  $1.55 M_{\odot}$  or heavier stars. The size of the effect may be

determined from Figure 1. In these calculations we assume  $\bar{K}/K_{\text{v}} = 1$ , but it is more like 0.1 beyond 13.6 eV at  $T_4 = 3$ . However, at  $T_4 = 6$ , the effect is small. Since for the  $1.4 M_{\odot}$  the bottom of the convection zone is at  $T_4 = 5.5$ , the Lyman jump will have little effect. However, in a  $1.55 M_{\odot}$  star, the bottom of the convection zone is at  $T_4 = 3.6$ . Elements which have lines beyond 13.6 eV only, will see their radiation force reduced by a factor of approximately 0.15. *When, in a star, the stable zone extends to  $T_4 \sim 3$ , the details of the atomic structure of each element will be important.* It is outside the scope of this paper to discuss this in detail, however, see the end of § IIa for a discussion of the effect of rare gas configuration on rare earth abundances.

The Lyman jump will be even more important for the  $2.0 M_{\odot}$  star in which the bottom of the convection zone is at  $T_4 = 1.6$ . We will, however, indicate which elements should be overabundant if we neglect the Lyman jump. We must remember that a few elements which we say here should be overabundant, actually will not be because of the Lyman jump. Generally all un-abundant elements should be overabundant unless affected by rare gas configurations. Because of rare gas configurations, Li, Na, Ar, K, Ca, Sr, and probably Ba will be underabundant. Helium and O will be underabundant because of saturation effects.

For the  $2.6$  and  $3.3 M_{\odot}$  stars we give on Figure 6 results at  $T_4 = 3$  since there is essentially no convection zone in those stars. The results for the  $5 M_{\odot}$  star would be larger by a factor of 2 than those for the  $3.3 M_{\odot}$  star. The radiation force on all un-abundant elements is here so large that, unless there are very strong ionization or Lyman jump effects, they will all be overabundant. Only those elements with large  $\chi_i/\chi_{i-1}$  (such as Eu, Gd, and U) can possibly see their radiation force reduced by more than one order of magnitude. All iron-peak elements except iron are strongly pushed upward.

### III. TIME SCALES FOR THE DEVELOPMENT OF ABUNDANCE ANOMALIES

We now show that, for most elements, the anomalies observed on Am or Ap stars pose no time scale problem. This result is firmly established. Indeed, in the lifetime of Am and Ap stars much larger anomalies than observed can be supplied by diffusion from the envelope of the star.

The time scales depend mainly on the size of the mixed zone in the outer region of the star (which in turn depends mainly on the effective temperature of the model; see the first paragraph of § II d) and on the radiation force below the mixed zone. In Am stars the mixed zone probably extends down to the bottom of the hydrogen convection zone (Vauclair, Vauclair, and Pamjatnikh 1974, Vauclair 1974, 1976). In Ap stars it is possible that the visible region of the star itself is stable. The time scales are then sometimes only of the order of years. In Michaud (1970) time scales were determined mainly for gravitational settling. But for overabundances of un-abundant elements (for which

radiation forces are large) time scales can be much shorter than the gravitational settling time scales.

A major simplification is possible for the calculations of the time evolution of abundance anomalies so long as equilibrium is not approached over a large fraction of the envelope. This is always an excellent approximation when turbulence is negligible as assumed in this paper. Then, in the diffusion equation, the concentration gradient is negligible and the diffusion velocity is independent of the local concentration (except in some cases through the radiation force). Consider the mass  $\Delta M_c$  (per  $\text{cm}^2$ ) of either the convection zone, in a star with an outer convection zone, or of the line-forming region, in a star without an outer convection zone. When an element of abundance  $X$  diffuses toward the center of the star, the mass  $\Delta M_c$  is being emptied through the bottom:

$$\frac{d}{dt}(X\Delta M_c) = +Xw_t, \quad (35)$$

where  $w_t$ , the diffusion velocity, is *negative* for downward diffusion, but constant in time since it does not depend on the abundance. Then we solve

$$X/X_0 = \exp[-t/\theta] \quad (36)$$

with

$$\begin{aligned} \theta &= -\Delta M_c / \rho w_t \\ &\approx +2.0 \times 10^{17} \Delta M_c Z^2 / AT_4^{3/2} (g_{\text{GT}} - g_R) \text{ (s)}, \end{aligned} \quad (37)$$

where  $g_R$  is the radiative acceleration calculated using equation (18),  $X_0$  is the abundance at  $t = 0$ , and  $g_{\text{GT}}$  is calculated using equation (8). Similarly for overabundances, when the concentration gradient term is negligible, the diffusion equation becomes a simple kinematic equation giving the velocity with which elements at a given point all move without feedback from the local concentration. The local concentration merely adjusts to keep the flow running. Instead then of solving the continuity and diffusion equations, it is much simpler, so long as the concentration gradient is negligible, to treat the diffusion equation as a kinematic equation and to calculate the time  $t_1$  it takes to bring to the atmosphere enough elements to create an overabundance  $c = X/X_0$ :

$$t_1(c) = \int_{r_1}^{r_c} \frac{dr}{w_t}, \quad (38)$$

where  $r_1$  is defined by

$$\frac{\Delta M(r_1)}{\Delta M_c} = \frac{X}{X_0}, \quad (39)$$

$X$  being the mass fraction of the element of interest and  $\Delta M(r_1)$  the mass (per  $\text{cm}^2$ ) above  $r_1$ . At  $t = 0$ , the star is assumed homogeneous with a natural abundance,  $X_0$ , of the element of interest. In other words, the overabundance at time  $t$  is the ratio of the mass of the zone from which elements have had time to migrate

to the convection zone (or line-forming region) to the mass of the convection zone (or line-forming region). The accuracy of this method was checked numerically for Hg against a detailed solution of the diffusion and conservation equations, and the effect of the approximation on all calculated time scales is less than 10 percent. The concentration gradient term is negligible in the diffusion velocity equation because the logarithmic pressure gradient term is multiplied by  $2A$ , and the logarithmic temperature gradient term by  $3.4Z^2$ , so that only for extremely large abundance anomalies is equilibrium ever approached. The concentration gradient term is important when equilibrium is approached; but equilibrium over 1 scale height of, say europium, would in an Ap star correspond to an overabundance of approximately  $10^{1000}$ !

For large overabundances to materialize, elements must be pushed upward from regions of the star where the temperature and density are very different from those at the surface. As elements move toward the surface, will they accumulate somewhere on the way, or will they all reach the surface? First, assume no ionization effect and that the lines are unsaturated. The flux of particles ( $\Gamma$ ) will be given by

$$\Gamma = X\rho D_t \frac{Ag_R}{kT} \propto X \frac{T^{1/2}}{Z^2}, \quad (40)$$

where equation (6) has been used and the expression for  $D_t$  has been taken from Aller and Chapman (1960) (see also Montmerle and Michaud 1976) neglecting the logarithmic term. Upward diffusion has been assumed dominant. From numerical calculations, for Mn, Sr, Eu, and Hg, it turns out that

$$Z \propto T^{1/2+\beta}, \quad (41)$$

where  $0 < \beta < 0.15$ .

In a steady state, elements do not accumulate on their way to the surface, so that  $\Gamma$  is independent of  $r$ . Equations (40) and (41) then give

$$X \propto T^{1/2+2\beta}$$

To maintain the flux when there is no saturation or ionization effect, the abundances decrease as  $T$  decreases toward the surface.

When the radiation force is saturated or when ionization effects are important, the situation is more complicated. Whenever they are important, the effects of accumulation of elements on the way to the surface are taken into account in the results presented below. In some cases they cause delays for elements like Mn and Cr. For the time evolution of the abundance of Mn in the atmosphere, two curves are shown on Figure 7b. The observed behavior of Mn should be between the two. The upper curve was calculated using radiation forces calculated assuming natural abundances of Mn at every point in the envelope; the lower curve, assuming 10 times a natural abundance. At the dips in its radiation force (such as those in Fig. 5a), Mn

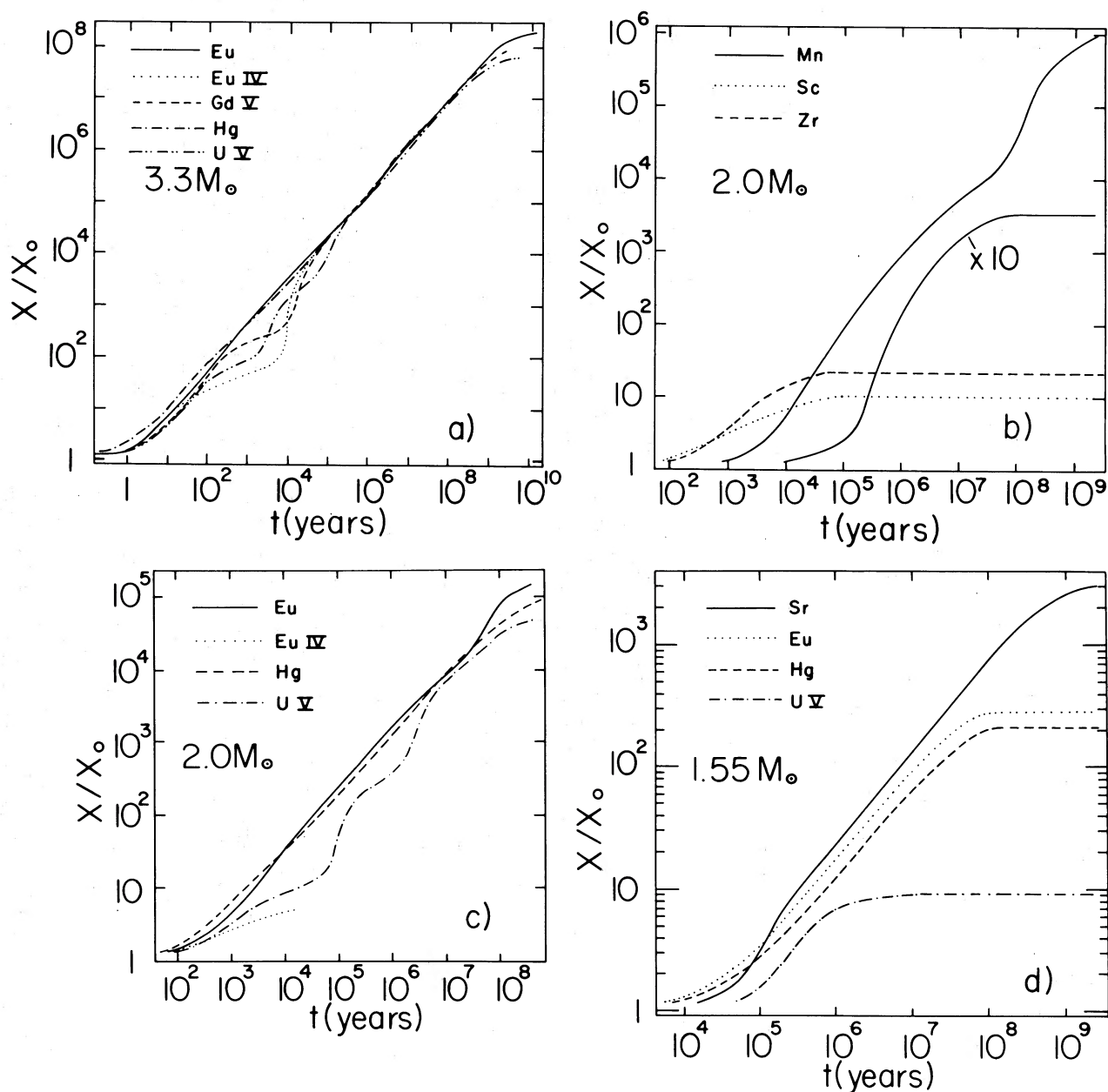


FIG. 7.—Time evolution of the abundances of a few elements of interest in the atmospheres of main-sequence stars with stable envelopes. In stellar lifetimes overabundances of up to seven, five, and two orders of magnitude can appear respectively in 3.3, 2.0, and 1.55  $M_{\odot}$  stars. Other cases are discussed in the text. On part (a) note that the time evolution is very regular except for Eu IV and U V whose abundances nearly stop increasing in the atmosphere after  $10^2$  years. Similarly on part (b) the abundances of Sc and Zr stop increasing after  $10^4$  years. This is due to the dips in the radiative acceleration described on Fig. 4 and 5. If the radiative acceleration is reduced below  $g_{GT}$  by the rare-gas configuration, the abundance stops increasing; if it is reduced but remains larger than  $g_{GT}$ , the abundance nearly stops increasing when elements coming from the point where  $g_R \sim g_{GT}$  reach the surface.

will accumulate, so that the flux can be carried. Because the calculated drop in the difference between the radiative force acceleration and  $g_{GT}$  is by a factor of 10, a tenfold increase in the abundance is needed. This leads to a slowdown of the diffusion. The effect is maximized by calculating (*lower curve*) the time evolu-

tion for 10 times a natural abundance of Mn everywhere. Results corresponding to the lower curve are always quoted here. Our estimate of the size of anomalies is then conservative. We now present the results, first for solar mass stars and then for more massive stars (see also Fig. 7).

TABLE 4  
DIFFUSION CHARACTERISTIC TIMES (years)

$M(M_{\odot})$	He	Mn	Ga	Sr	Eu	Hg
2.6.....	$4.3 \times 10^4$	...	...	...	...	...
2.0.....	$1.3 \times 10^5$	...	...	$9.2 \times 10^9$	...	...
1.55.....	$1.8 \times 10^6$	...	$1.9 \times 10^6$	...	...	...
1.4.....	$4.3 \times 10^6$	...	...	...	...	...
1.2.....	$1.1 \times 10^8$	$1.9 \times 10^8$	$3.6 \times 10^8$	$1.6 \times 10^8$	$8.0 \times 10^7$	$5.2 \times 10^7$
1.07.....	$1.5 \times 10^9$	$3.2 \times 10^9$	$2.9 \times 10^9$	$2.5 \times 10^9$	$2.2 \times 10^9$	$1.9 \times 10^9$
1 ( $\alpha = 1.5$ ).....	...	$2.1 \times 10^{10}$	$2.0 \times 10^{10}$	$1.9 \times 10^{10}$	$1.7 \times 10^{10}$	$1.5 \times 10^{10}$
1 ( $\alpha = 1.0$ ).....	$5.4 \times 10^9$	$5.1 \times 10^9$	$4.9 \times 10^9$	$4.4 \times 10^9$	$3.8 \times 10^9$	$3.4 \times 10^9$
1 ( $\alpha = 0.7$ ).....	...	$5.3 \times 10^8$	$4.4 \times 10^8$	$3.9 \times 10^8$	$3.4 \times 10^8$	$2.6 \times 10^8$

In solar-type stars, diffusion leads to underabundances (see § II*d*). One may then use equations (36) and (37) to calculate the abundance anomalies in the convection zone and so in the atmosphere. The time scales are listed in Table 4 for a few elements of interest. Whether large abundance anomalies should appear or not on the surface of solar-type stars depends entirely on the ratio of mixing length to pressure scale height and will be settled only by progress in convection theories. For  $\alpha = 1.5$ , 1.0, and 0.7 the abundance anomalies should, for Mn, respectively be by factors of 0.8, 0.4, and  $2 \times 10^{-4}$  after  $4.5 \times 10^9$  years. The relative homogeneity of abundances in solar mass stars may perhaps be used to set a lower limit on  $\alpha$ ; however, meridional circulation must also be taken into account (Vauclair, Vauclair, and Michaud, in preparation). Perhaps the light elements (Li, Be, B) will be very useful in this respect (Vauclair, Vauclair, Schatzman, and Michaud, in preparation).

For the  $1.07 M_{\odot}$  model, the results quoted are for an  $\alpha = 1$  model and do depend on  $\alpha$ ; however, abundance anomalies appear here most likely to materialize. Note that the heaviest elements will be most underabundant and that the expected underabundances are of many orders of magnitude. That holds even more strongly for the  $1.2 M_{\odot}$  stellar model, though there some of the elements will *probably* be overabundant. The underabundances will be by very large factors ( $10^{-6}$  for Hg after  $10^9$  years; the reader can easily calculate cases of interest to him by using equation [36]). The possible overabundances of Be, B, and P, however, will not be larger than a factor of 10, whereas those of F, Na, Cl, K, Sc, Ti, and V will be smaller than a factor of 3. The other elements either are likely to be underabundant or are certainly underabundant (see § II*d*).

In a  $1.4 M_{\odot}$  star, diffusion leads, in the convection zone and so in the atmosphere, to overabundances by two orders of magnitude for elements with  $60 < A < 100$  and for F, Cl, K, and Sc; but by one order of magnitude above  $A = 100$  and for P, A, Ca, V, Cr, Mn, Co, and Ni. In this and other stars, the quoted overabundances are uncertain by about one order of magnitude for individual elements.

In  $1.55 M_{\odot}$  stars, diffusion leads to overabundances by three orders of magnitude for elements with  $60 < A < 100$  and for F and K; but by two orders of magnitude for elements with  $A > 100$  and for Cl, Cr,

Mn, Co, and Ni. Overabundances by a factor of 3 are expected for Zr, and by a factor of 10 for B, P, Ar, Ti, V, Nb and Mo. Note that here strontium is overabundant by three orders of magnitude. Yttrium is underabundant by many orders of magnitude, and zirconium is overabundant by a factor of 3. This is due to the state of ionization at the bottom of the convection zone. Note also from Table 4 that the disappearance of helium is very rapid: it takes only  $10^6$  years.

In  $2 M_{\odot}$  stars, overabundances will be by factors of 3 for Be, Sc, Y, and Al; of 10 for B, Ti, and Zr; of 100 for P and V; of 1000 for Cl, Cr, Mn, Co, and Ni; and of  $10^5$  for F and those elements above the iron peak not specifically mentioned. But look at Figure 6 for underabundant elements. Note the behavior of Sr, Y, and Zr. In smaller stars the maximum overabundances were determined by the point where

$$g_R = g_{GT}.$$

Elements could not be more than 1000 times overabundant in a  $1.55 M_{\odot}$  star because at the point in the envelope where  $\Delta M = 1000 \Delta M_c$ , the radiative acceleration becomes smaller than  $g_{GT}$ . However, in a  $2 M_{\odot}$  star, this point occurs so deep in the star that elements do not have time to diffuse from there to the surface in the stellar lifetime (see Fig. 7). In  $2 M_{\odot}$  and heavier stars, the maximum size of the overabundances are determined by the stellar lifetime.

In  $2.6 M_{\odot}$  stars, there are overabundances by a factor of 3 for Y; of 10 for Be, Al, Zr, and Sc; of  $10^2$  for B, Ti, and Nb; of  $10^3$  for P, Ar, and V; of  $10^4$  for Cl, K, Cr, Mn, Co, and Ni; of  $10^5$  for F; and of  $10^6$  for those elements above the iron peak that are overabundant (see Fig. 6) but not mentioned above. The limit of  $10^6$  is due to the time it takes for elements to diffuse upward. For the  $2.6 M_{\odot}$  and lighter stars we assumed that  $\Delta M_c$  included the mass of the hydrogen convection zone. However in the  $2.6 M_{\odot}$  star, the convection carries little energy and could probably be suppressed by the magnetic field. Then the outer atmosphere of the star would be stable, the zone that one needs to contaminate is only the line-forming region, and the overabundances would generally be multiplied by a factor of 10. In the  $3.3$  and  $5.0 M_{\odot}$  stars, only the line-forming region is assumed contaminated.

In  $3.3 M_{\odot}$  stars, there will be overabundances by a factor of 3 for Be, Mg, S, and Ca; of 10 for B, N, Al,

Sc, Sr, and Y; of  $10^2$  for Ti and Zr; of  $10^3$  for P and V; of  $10^4$  for Cl and Cr; of  $10^5$  for F, Mn, Co, and Ni; and of  $10^7$  for most of the elements above the iron peak. Here the mass of the contaminated zone,  $\Delta M_c$ , is assumed to be the mass of the line-forming region that is the region above  $\tau_{\text{Rosseland}} = 0.1$ . This is somewhat approximate. If one preferred a larger line-forming region by a factor  $L$ , one merely would decrease the overabundances by the same factor since the number of diffused elements would not be changed but would be mixed in a larger mass.

In a  $5 M_{\odot}$  star we have very nearly the same thing: Be, Mg, Sc, Fe, and Y overabundant by a factor of 3; B, N, Al, Si, S, Zn by a factor of 10; Ti by  $10^2$ ; P and V by  $10^3$ ; Cl, Cr, and Mn by  $10^4$ ; F, Co, and Ni by  $10^5$ ; and most of the elements above the iron peak by  $10^7$ . Note that especially in the last three stars, the small abundances ( $\leq 10$ ) are entirely caused by diffusion at temperatures smaller than 40,000 K where our results are uncertain. Some of those calculated overabundances are then expected not to materialize. However, there is no doubt that overabundances of P, V, Cl, Cr, Mn, F, Co, and Ni by four orders of magnitude or so are allowed by the reservoir. For most of the elements above the iron peak, it is seven orders of magnitude.

#### IV. DISCUSSION

Compare now these results with observed abundance anomalies (Preston 1974). The Am stars correspond approximately to our 1.55 and  $2.0 M_{\odot}$  stars. Diffusion leads to overabundances of three to five orders of magnitudes for heavy elements in those stars, whereas overabundances of one to two orders of magnitude are observed. Similarly, underabundances of Ca, Sc, and a few light elements are predicted by diffusion (see Fig. 6) and are observed, but the predicted underabundance factors are much larger than observed. We assumed, in our calculations, no turbulence or meridional circulation. Either would considerably diminish the anomalies predicted by diffusion. Observations seem to tell us that some stars are stable enough for diffusion to be important but that they are barely stable enough, the abundance anomalies being considerably reduced by turbulence or meridional circulation. The effects of turbulence and meridional circulation will be studied by us in a separate paper (Vauclair, Vauclair, and Michaud, in preparation). A detailed comparison with observations must await

these results. Similarly, the lower temperature stars ( $T_{e4} \approx 0.6$ ) are here predicted to have overabundances of about one order of magnitude, but the same turbulence or meridional circulation that reduces the anomalies in Am stars probably reduces them to a factor of 3 or lower at  $T_{e4} = 0.6$ . The predicted underabundances, which are often by very large factors in low-mass stars, may not be eliminated and should be looked for. In more massive stars ( $M \geq 2.5 M_{\odot}$ ) our results should be compared with observations of Ap and Bp stars. Here the predicted anomalies are slightly larger ( $10^7$  instead of  $10^6$ ) than the largest observed abundance anomalies. These calculations show clearly, beyond the error bars, that even the largest observed abundance anomalies can be caused by the migration of elements from the interior of the star. However, our treatment of the atmosphere is here too approximate for us to carry a detailed element-by-element comparison in Ap stars. The atmosphere will modulate the abundance anomalies.

As a final remark, we would like to point out where more calculations are needed and where the calculations presented here are accurate enough. In general, at  $T_4 \lesssim 4$ , the calculations presented here are not accurate enough. They do give the average behavior, but many individual elements (e.g., some of the rare earths) are expected to behave very differently from the average. Detailed studies are then needed. However, at  $T_4 \gtrsim 4$ , the reverse is true. Most elements are expected to behave like the average. In particular, no difficulty is expected from iron-peak or heavier elements. Detailed studies may be needed at temperatures larger than  $T_4 \approx 4$  for some of the lighter elements: for Li, Be, and B certainly, perhaps for Si and a few others. For most elements, then, detailed atomic data ( $f$ -values, energy of excited levels, ionization energy) are needed only for calculations at  $T_4 \lesssim 4$ , corresponding to states of ionization with ionization potentials of 60 eV or less. Such data are not always available, but even fewer data exist for more ionized states.

We are indebted to Dr. A. N. Cox for kindly calculating opacities for us and for supplying them to us in an especially useful form. We thank Drs. Claude Mégessier, Thierry Montmerle, Françoise Praderie, and Myron Smith for a critical reading of the manuscript. We would like to thank Alice Chénard for the typing of a difficult manuscript and Robert Martel for the drawings.

#### APPENDIX A

##### ESTIMATE OF $f$ -VALUES

We based our estimates of  $f$ -values mainly on the analysis and Tables of Wiese, Smith, and Glennon (1966) and Wiese, Smith, and Miles (1969). They so depend implicitly on experimental and theoretical evaluations.

In their analysis Wiese, Smith, and Miles (1969) give the  $Z$ -dependence (where  $Z$  is the charge of the nucleus whereas elsewhere in this paper  $Z$  is the charge of the ion) of transition probabilities and  $f$ -values for a number of configurations (see in particular their Figs. 10–21). As  $Z$  increases, the  $f$ -values of the lines connecting some configurations go up while others go down. This is to be expected from the sum rule (Pecker and Schatzman 1959)

TABLE A1  
OSCILLATOR STRENGTHS

State (1)	$\sum_n f_{nm}$ (2)	$(1 \leq f)$ (3)	$(0.3 < f \leq 1)$ (4)	$0.1 < f \leq 0.3$ (5)	$10^{-2} < f \leq 10^{-1}$ (6)	$10^{-3} \leq f < 10^{-2}$ (7)	$f < 10^{-3}$ (8)
Ground states . . . . .	0.70	0.12	0.5	1.12	0.9	0.6	0.5
First excited states . . .	0.75	0	0.9	1.25	1.9	0.9	1.8
8 states of Si I . . . . .	0.57	0	0.5	1.4	2.1	2.1	1.1
10 states of Si II . . . . .	0.78	0.2	0.6	0.8	1.1	0.7	0.9
14 states of Si III . . . . .	1.37	0.7	0.9	1.9	0.9	0.07	0.14
11 states of Si IV . . . . .	1.15	0.4	1.0	0.8	1.6	0.9	0.09
Average (all) . . . . .	0.89	0.24	0.73	1.2	1.4	0.88	0.76
Average (Si) . . . . .	0.97	0.43	0.83	1.2	1.2	0.56	0.38
Chosen middle . . . . .	1.0	...	$1 \times 0.5112$	$2 \times 0.2$	$4 \times 0.02$	$4 \times 0.002$	$4 \times 0.0002$
Chosen low . . . . .	0.2	...	...	$1 \times 0.1$	$2 \times 0.04$	$4 \times 0.004$	$4 \times 0.0004$
Chosen high . . . . .	2.0	...	...	$10 \times 0.10$	$20 \times 0.04$	$40 \times 0.004$	$40 \times 0.0004$

which relates the algebraic sum of the  $f_{nm}$ -values from level  $n$  to all other levels, to the number of outer electrons involved in the state  $n$  (Unsöld 1955, p. 350). As  $Z$  varies, the number of electrons involved in a given configuration does not change. For this reason, the "average"  $f$ -values will be determined by an analysis of a number of ions in Wiese, Smith, and Miles (1969), and upper and lower limits will also be justified. Then the  $f$ -values so determined will be compared with the experimental ones for Fe I.

In Table A1 we have summarized the information from Wiese, Smith, and Miles (1969) used in this paper. We have summed, from a given lower level  $m$ , the  $f_{nm}$ -values of transitions to all upper levels within 80 percent of the ionization potential of the lower level. Beyond that energy the flux available drops down too rapidly for the transitions to contribute (see Fig. 1). These are given in column (2). We have also given, in succeeding columns, the average number of transitions from one lower level, in a given range of  $f$ -values. The averages were carried out separately from the ground states of neutral elements from Na to Ar, for the first excited states of the same elements, and for eight to 14 levels of the first four ionization states of Si. Silicon was singled out since we also could compare the data with the more complete tables of Moore (1965) for the intensity of spectral lines. This comparison suggested to stop our averages after the tenth level of Si II, the 14th of Si III, and the 11th of Si IV since the data of Wiese, Smith, and Miles (1969) were becoming less complete. We similarly limited the study to the ground states and first excited states of the neutral elements.

From a comparison of the various ionization states of Si (which cover the Na I to Si I configurations) we conclude that the total  $f$ -value from lower levels does *not* depend considerably on the number of outside electrons. The sum always appears reasonably close to 1. We estimate a lower value of 0.2 and an upper value of 2.0. We have also compared these values with those of Fe I (not shown on Table A1) (Allen 1971; Corliss and Warner 1964). Again, after the recent correction (Allen 1971) the average  $f$ -values summed to all upper states but *averaged* over all lower states is close to 1. We have not included these data because of some arbitrariness as to exactly how to introduce the corrections. The average  $f$ -value we need here then does not increase with the number of electrons outside closed shells (the sum rule, Unsöld 1955). It appears more related to the number of electrons that can make the transitions, and this is always reasonably close to 1. This is the value chosen for all unsaturated calculations and for the "middle" estimate of saturated calculations.

For saturated calculations the number of transitions is also important. This is estimated from columns (3)–(8). The number of strong transitions ( $f > 10^{-1}$  and perhaps  $f > 10^{-2}$ ) can be reasonably estimated from the data we present. But the number of weak transitions ( $f < 10^{-2}$ ) is clearly underestimated because not all weak transitions have been observed. Furthermore, in our analysis of the Fe I spectrum, whereas it appeared that the summed  $f$ -value remained constant, the number of transitions contributing to it increased considerably. Finally, from equation (6) it appears that, for an element with  $A = 16$  if  $T_{e4} = T_4 = 1$ , one unsaturated transition with  $f = 10^{-3}$  leads to  $g_R = 10^4 \text{ cm s}^{-2}$  and so is sufficient to push the element upward. Only the weak transitions, from a given lower level, whose summed  $f$ -value is  $\sim 10^{-3}$  will contribute significantly to the radiation force. Those arguments have led us to choose the middle, low, and high estimates shown in Table A1. Only those results which are independent of the estimate of the number of lines and of the  $f$ -value will be given a high degree of certainty.

## APPENDIX B

### EXAMPLE OF RADIATIVE ACCELERATION CALCULATIONS

As an example of how radiative accelerations can be calculated from the equations obtained here, the strontium radiative acceleration is calculated at two points in a  $2.6 M_{\odot}$  stellar envelope. First at  $T_4 = 10$ , from equation (10)

and Table 2,  $\Delta M/M = 4 \times 10^{-8}$ , so that we can compare our result with those on Figure 4b. Then calculate the state of ionization of Sr. Using equation (11), with  $N_i/N_{i-1} = 1$ , and  $B_{i-1}/B_i = 1$ , we find  $\chi_{i-1} = 111$  eV. From Carlson *et al.* (1970), strontium is then mainly in the form of Sr VII and Sr VIII, which are not rare-gas configurations. One immediately obtains  $g_R = 2.6 \times 10^5$  cm s $^{-2}$  from equation (6) ( $A = 88$ ).  $T_{e4}$  was taken from Table 1, and  $r = R$  was assumed. The correction for saturation can be obtained using equation (30), with  $\bar{K} = 10$ . More accurate values for  $\bar{K}$  could be obtained from a stellar envelope model, but we checked that  $\bar{K} = 10$  is a good enough approximation for nearly all cases. Then using "natural" abundances for Sr [ $X(\text{Sr}) = 7.35 \times 10^{-8}$ ], one obtains from equation (30)  $g_{Rs} = 2.5 \times 10^5$  cm s $^{-2}$ . This value for the upward radiative acceleration should be compared with the downward acceleration of equation (8). Using values from Table 1 one obtains  $g_{GT} = 1.70 \times 10^4$  cm s $^{-2}$ , so the correction for thermal diffusion is only 13 percent in this case. The radiative acceleration on Sr is much larger than the downward acceleration at  $T_4 = 10$ .

Now calculate the radiation force on Sr at  $T_4 = 3$ , even though our formulae are not so accurate there. From equation (11), we calculate  $\chi_{i-1} = 39$  eV, which from Carlson *et al.* (1970) implies that Sr is partially in a rare-gas configuration. It is then necessary to calculate the fraction of Sr that is in the rare-gas configuration. From equation (11), again with  $\chi_{i-1} = 41.31$  eV,  $B_i/B_{i-1} = 1$ , we obtain

$$\frac{N(\text{Sr IV})}{N(\text{Sr III})} = 0.4.$$

We calculate only the unsaturated force:

$$g_R = 0.7 g_R(\text{Sr III}) + 0.3 g_R(\text{Sr IV}).$$

The radiation force on Sr IV is obtained from equations (19) and (21), while that on Sr III, a rare-gas configuration, must be corrected as specified in equations (19) and (20). For Sr III:

$$u_{rg} = 0.6 \times 41.3/kT = 9.6.$$

And from Figure 1

$$P(9.6) = 0.6,$$

so that

$$\begin{aligned} g_R &\approx [(0.7 \times 0.6 + 0.3 \times 0.2)/3] \times 1.7 \times 10^8 T_{e4}^4 / AT_4 \\ &= 1.4 \times 10^5 \text{ cm s}^{-2}. \end{aligned}$$

Because of the rare-gas configuration, the radiation acceleration is reduced by a factor of 6, in reasonable agreement with the more exact calculation shown on Figure 4b (eq. [10] gives  $\Delta M/M = 2.7 \times 10^{-10}$ ). Note that in this Appendix we neglected the effect described in equation (18), but that it was included in the calculations of Figure 4b. Except when the element is neutral or once ionized, it can be neglected in first approximation.

## APPENDIX C

### EFFECT OF SATURATION

We will first show how to arrive at equation (30) which evaluates the effect of saturation on radiative accelerations. We will obtain a function with three arbitrary parameters. They will be determined by comparison with "exact" calculations for manganese.

Assume that the radiation flux in two Doppler widths is transmitted to element  $A$  via one line. Then from equation (1)

$$g_S = 2F_\nu(A)\Delta\nu_D = g_{RI} \left[ 5.5 \times 10^{-12} \frac{\bar{K} A^{1/2} T_4^{3/2}}{X(A)} \right], \quad (\text{C1})$$

where  $\Delta\nu_D$  and  $g_{RI}$  were taken respectively from equations (27) and (6). Since we assumed that *all* the radiation flux in  $2\Delta\nu_D$  was transmitted to element  $A$ , we used

$$K_\nu(A) = K_\nu$$

in equation (1). We further assumed  $P(u) = 3$  and  $u = 5$  following the same argumentation that led to equation (6). Equation (C1) gives the amount of radiative acceleration transmitted to element  $A$  through one single saturated

line of Doppler width. As the abundance of element  $A$ ,  $X(A)$ , increases, the saturated width of one line will increase and the number of saturated lines will increase. We approximate this behavior by multiplying the right-hand side of equation (C1) by  $B'$ ,

$$B' = B_0[1 + X^k/X_0^k],$$

where  $B_0$ ,  $X_0$ , and  $k$  are arbitrary constants to be determined later. Then

$$g_{RIs} = 5.5 \times 10^{-12} B' g_{RI} \frac{\bar{K}A^{1/2}T_4^{3/2}}{X(A)}. \quad (C2)$$

The saturated radiation force must equal the unsaturated radiation force,  $g_{RI}$ , in the limit of small abundances. We then use the simple interpolation formula:

$$g_{RIs} = g_{RI} \frac{5.5 \times 10^{-12} B' \bar{K}A^{1/2}T_4^{3/2}}{5.5 \times 10^{-12} B' \bar{K}A^{1/2}T_4^{3/2} + X(A)}, \quad (C3)$$

which has the required behavior in the two limits of small and large abundances. We have determined  $B_0$ ,  $X_0$ , and  $k$  by comparing  $g_{RIs}$  with radiation forces calculated for Mn, as described in § IIb. We then rewrote  $g_{RIs}$  in the slightly simpler but equivalent form of equations (30) and (31). The constant  $E$  is introduced so that  $g_{RIs}$  goes to the proper limit for the "high" and "low" approximations.

#### REFERENCES

- Allen, C. W. 1963, *Astrophysical Quantities* (London: Athlone Press).  
 ———. 1971, *M.N.R.A.S.*, **152**, 295.  
 Aller, L. H., and Chapman, S. 1960, *Ap. J.*, **132**, 461.  
 Burgers, J. M. 1960, in *Plasma Dynamics*, ed. F. H. Clauser (Reading: Addison-Wesley).  
 Cameron, A. G. W. 1973, in *Explosive Nucleosynthesis*, ed. D. N. Schramm and W. D. Arnett (Austin: University of Texas Press).  
 Carlson, T. A., Nestor, C. W., Wasserman, N., and McDowell, J. D. 1970, *Atomic Data*, **2**, 63.  
 Chapelle, J., and Sahal-Bréchet, S. 1970, *Astr. and Ap.*, **6**, 415.  
 Corliss, C. H., and Warner, B. 1964, *Ap. J. Suppl.*, **8**, 395.  
 Cowley, C. R., and Day, C. A. 1976, *Ap. J.*, **205**, 440.  
 Cox, A. N. 1965, in *Stellar Structure*, Vol. 8 of *Stars and Stellar Systems*, ed. L. H. Aller and D. B. McLaughlin (Chicago: University of Chicago Press).  
 Cox, A. N., and Stewart, J. N. 1970, *Ap. J. Suppl.*, No. 174, **19**, 243.  
 Griem, H. R. 1960, *Ap. J.*, **132**, 883.  
 Herzberg, G. 1944, *Atomic Spectra and Atomic Structure* (New York: Dover).  
 Kelly, R. L., and Harrison, D. E., Jr. 1971, *Atomic Data*, **3**, 177.  
 Kobayashi, M., and Osaki, Y. 1973, *Pub. Astro. Soc. Japan*, **25**, 495.  
 Martel, G. 1974, Internal Report, Université de Montréal.  
 Michaud, G. 1970, *Ap. J.*, **160**, 641.  
 ———. 1973, *Ap. Letters*, **15**, 143.  
 ———. 1975, *IAU Colloquium No. 32*, Vienna.  
 Michaud, G., Reeves, H., and Charland, Y. 1974, *Astr. and Ap.*, **37**, 313.  
 Michaud, G., and Vauclair, S. 1972, *Ap. Letters*, **11**, 117.  
 Mihalas, D. 1965, *Ap. J. Suppl.*, **9**, 321.  
 Montmerle, T., and Michaud, G. 1976, *Ap. J. Suppl.*, **31**, 489.  
 Moore, C. E. 1949, *Atomic Energy Levels* (NBS Pub., No. 467, Vol. 1).  
 ———. 1952, *Atomic Energy Levels* (NBS Pub., No. 467, Vol. 2).  
 ———. 1958, *Atomic Energy Levels* (NBS Pub., No. 467, Vol. 3).  
 ———. 1965, *Selected Tables of Atomic Spectra* (NSRDS-NBS 3, §1).  
 Paczynski, B. 1969, *Acta Astr.*, **19**, 1.  
 Pecker, J. C., and Schatzman, E. 1959, *Astrophysique Générale*, (Paris: Masson et Cie, editeurs).  
 Preston, G. W. 1974, *Ann. Rev. Astr. and Ap.*, **12**, 257.  
 Sahal-Bréchet, S., and Segre, E. R. A. 1971, *Astr. and Ap.*, **13**, 161.  
 Smith, M. A. 1971, *Astr. and Ap.*, **11**, 325.  
 ———. 1973, *Ap. J. Suppl.*, **25**, 277.  
 ———. 1974, *Ap. J.*, **189**, 101.  
 Spitzer, L. 1968, *Diffuse Matter in Space* (New York: Interscience).  
 Unsöld, A. 1955, *Physik der Sternatmosphären* (2nd ed.; Berlin: Springer-Verlag).  
 Vauclair, G., Vauclair, S., and Pamjatnikh, A. 1974, *Astr. and Ap.*, **31**, 63.  
 Vauclair, S., Michaud, G., and Charland, Y. 1974a, *Astr. and Ap.*, **31**, 381.  
 Vauclair, G. 1974, Journées d'Etude sur les Binaires Serrées, Nice.  
 ———. 1976, *Astr. Ap.*, **50**, 435.  
 Watson, W. D. 1970, *Ap. J. (Letters)*, **162**, L45.  
 ———. 1971a, *Astr. and Ap.*, **13**, 263.  
 ———. 1971b, *Nature Phys. Sci.*, **229**, 228.  
 Wiese, W. L., Smith, M. W., and Glennon, B. M. 1966, *Atomic Transition Probabilities*, Vol. 1 (NSRDS-NBS 4).  
 Wiese, W. L., Smith, M. W., and Miles, B. M. 1969, *Atomic Transition Probabilities*, Vol. 2 (NSRDS-NBS 22).

YVES CHARLAND and GEORGES MICHAUD: Dép. de Physique, Université de Montréal, Case postale 6128, Montréal 101, P. Québec, Canada

GÉRARD VAUCLAIR and SYLVIE VAUCLAIR: D.A.F., Observatoire de Meudon, Meudon, France